Corrosion Science 177 (2020) 108993

Contents lists available at ScienceDirect

Corrosion Science

journal homepage: www.elsevier.com/locate/corsci

Distinguishing two different microbiologically influenced corrosion (MIC) mechanisms using an electron mediator and hydrogen evolution detection

Di Wang [a], Jialin Liu [a], Ru Jia [a], Wenwen Dou [b,*], Sith Kumseranee [c], Suchada Punpruk [c], Xiaogang Li [d], Tingyue Gu [a,*]

[a] Department of Chemical and Biomolecular Engineering, Institute for Corrosion and Multiphase Technology, Ohio University, Athens, OH 45701, USA
[b] Department of Materials Science and Engineering, Ocean University of China, Qingdao 266100, China
[c] PTT Exploration and Production, Chatuchak, Bangkok 10900, Thailand
[d] Corrosion & Protection Center, University of Science & Technology Beijing, Beijing 100083, China

ARTICLE INFO

Keywords:
Microbiologically influenced corrosion
Extracellular electron transfer
Sulfate reducing bacteria
Riboflavin
Carbon steel
Copper

ABSTRACT

Carbon steel MIC (microbiologically influenced corrosion) and copper MIC by *Desulfovibrio vulgaris* (a sulfate reducing bacterium) were shown to behave very differently. Carbon steel MIC was accelerated with an 84 % weight loss increase by 20 ppm (w/w) riboflavin (an electron mediator) while Cu MIC was not. This was because the former belongs to extracellular electron transfer (EET)-MIC while the latter metabolite (M)-MIC. Cu MIC by biogenic H_2S yielded a large amount of H_2. This work proved that an electron mediator can distinguish EET-MIC from M-MIC, and H_2 gas detection is very sensitive in identifying M-MIC with H_2 evolution.

1. Introduction

It is widely viewed that microbiologically influenced corrosion (MIC) is now a pervasive problem in many fields such as the oil and gas industry, water utilities, and sometimes biomedical implants [1,2]. Sulfate is a ubiquitous electron acceptor (oxidant) in anaerobic environments [3]. Thus, sulfate reducing bacteria (SRB) are prevalent in anaerobic environments to take advantage of the presence of this electron acceptor for respiration.

In a corrosive environment such as an oil and gas pipeline with CO_2 corrosion, microbial biofilms can damage the partially passivating siderite mineral film, thus accelerating CO_2 corrosion [4]. Apart from influencing the corrosion by other corrosive agents, biofilms can cause corrosion by themselves in the absence of a pre-existing corrosion factor. This kind of corrosion has been the main focus in mechanistic MIC investigations. Under anaerobic condition, the mechanisms for MIC caused by biofilms can be classified into two distinct categories [5]. In the first type, biofilms transport electrons from extracellular iron oxidation across the cell wall to reach the cytoplasm where the reduction of an exogenous electron acceptor such as sulfate happens [6,7]. Cross-cell wall electron transfer is also called extracellular electron transfer (EET) [8,9]. Thus, this type MIC is known as EET-MIC in MIC science [10,11]. SRB MIC and NRB (nitrate reducing bacteria) MIC of carbon steel are typical examples of EET-MIC [12]. The corrosion of carbon steel by a *Shewanella* sp. using fumarate as terminal electron acceptor also belongs to EET-MIC [13].

In EET-MIC, biofilms harvest energy from energetic metals in their respiration. The following two electrochemical reactions can be used to explain the bioenergetics of MIC in SRB respiration for energy production when sulfate is the terminal electron acceptor [14–16].

$$4Fe \rightarrow 4Fe^{2+} + 8e^{-} \quad (E^{\circ} = -447\ mV) \tag{1}$$

$$SO_4^{2-} + 9H^{+} + 8e^{-} \rightarrow HS^{-} + 4H_2O \quad (E^{\circ\prime} = -217\ mV) \tag{2}$$

Because an iron or steel matrix is insoluble, extracellularly released electrons in Reaction (1) must be transported to the SRB cytoplasm via EET for use in Reaction (2) that requires intracellular biocatalysis. $E^{\circ\prime}$ in bioelectrochemistry is defined as the reduction potential (vs. standard hydrogen electrode) at 25 °C, pH 7 (indicated by the apostrophe in E), and 1 M solutes (or 1 bar partial pressure for gases) excluding H^{+}. The cell potential ($\Delta E^{\circ\prime}$) of the redox reaction combining the two half reactions above at these conditions is +230 mV. This positive potential means the redox reaction of iron oxidation coupled with sulfate reduction has a negative Gibbs free energy change, indicating that the reaction is thermodynamically favorable or energy is released [12].

The bisulfide product in Reaction (2) can gain one proton to become

* Corresponding authors.
E-mail addresses: dww@ouc.edu.cn (W. Dou), gu@ohio.edu (T. Gu).

https://doi.org/10.1016/j.corsci.2020.108993
Received 6 May 2020; Received in revised form 21 July 2020; Accepted 2 September 2020
Available online 6 September 2020
0010-938X/

H_2S or to lose one proton to become S^{2-} depending on broth pH [17],

$$HS^- + H^+ \rightarrow H_2S \quad (3)$$

$$HS^- \rightarrow H^+ + S^{2-} \quad (4)$$

H_2S is secreted by SRB into the surrounding broth. Its dissociation reactions release HS^- (dominant sulfide species), S^{2-} and H^+ in the broth [16]. The amount of S^{2-} is negligible if pH is not very high [3]. H_2S can be corrosive, but it is not a significant contributor to carbon steel MIC caused by SRB at near neutral pH [14]. Using the same broth volume with different headspace volumes in anaerobic vials, Jia et al. [10] showed that a larger headspace allowed more H_2S to escape to the headspace. As a consequence, the dissolved H_2S concentration in the broth was lower, resulting in less H_2S toxicity and a higher sessile *Desulfovibrio vulgaris* cell count which caused more severe carbon steel MIC. Using a different experimental design with fixed broth and headspace volumes, Jia et al. [18] showed that adding more Fe^{2+} to the culture medium helped to detoxify H_2S toxicity, resulting in better *D. vulgaris* planktonic and sessile growth and thus a higher dissolved H_2S. As a consequence of a high sessile SRB cell count, more severe carbon steel MIC occurred. In these two studies, the dissolved H_2S concentrations shifted in opposite directions, one lower and one higher, when headspace volume and Fe^{2+} concentration were increased. However, both led to more severe corrosion. In both cases, the sessile cell count increased, which is consistent with EET-MIC, because more sessile cells harvest more electrons [3].

There are two different electron transfer methods for EET from a metal surface to a cell's outer surface. One is direct electron transfer (DET) [19,20], which means that a direct contact between microorganisms and the iron surface is required. The other is mediated electron transfer (MET) [21,22] involving soluble redox mediators. SRB species such as *Desulfovibrio ferrophilus* have redox-active outer membrane bound *c*-type cytochromes (OMCs), homologous to those in *Shewanella* and *Geobacter*, which are capable of utilizing soluble electron mediators such as riboflavin as electron shuttles [23,24]. The *D. vulgaris* genome lacks the genes coding for such OMCs. However, different OMCs were discovered recently by a group at NIMS in Japan [25]. *D. vulgaris* is already well known for electro-active *c*-type cytochromes in its periplasmic space for electron transfer inside the cell [25]. Furthermore, hydrogenase-positive SRB species such as *D. vulgaris* are capable of hydrogen-cycling [26]. At different locations in an SRB cell, hydrogenase enzymes can convert H^+ into H_2 with electron uptake and then converts H_2 back to H^+ with electron release [27]. This so-called hydrogen-cycling is actually mediated electron transfer using the $2H^+/H_2$ shuttle, which is rather "universal" among microbes [28].

Flavodoxin plays an important role in *D. vulgaris* electron transfer [29]. Flavin mononucleotide (FMN), or riboflavin-5′-phosphate, is a biomolecule produced from riboflavin by the enzyme riboflavin kinase [30]. OMCs in various bacterial species are known to be involved in EET. They are capable of interacting with soluble electron shuttles such as riboflavin [23]. The electron transport chain (ETC) inside SRB cells also rely on membrane-bound and dissolved redox mediators to shuttle electrons [31]. Riboflavin can promote the overall electron transfer process in EET-MIC [32].

It has been shown that electron transfer for the uptake of extracellular electron is rate limiting in SRB MIC of C1018 carbon steel and 304 stainless steel which belongs to EET-MIC [15,33]. The addition of 10 ppm (w/w) of either riboflavin or flavin adenine dinucleotide (FAD) accelerated carbon steel and stainless steel weight losses in anaerobic vials with SRB [15,34]. Similarly, these two electron transfer mediators have been found to accelerate the MIC of C1018 carbon steel caused by nitrate reducing *Pseudomonas aeruginosa* [33]. Recently, Huang et al. [35] manipulated the *PhzH* gene that encodes an electron mediator in *P. aeruginosa*. They found that the gene's deletion (knockout) greatly reduced the MIC of 2205 duplex stainless steel by *P. aeruginosa*, while its restoration in the knockout strain largely restored the microbe's corrosion ability [35].

Both NRB MIC and SRB MIC against carbon steel and stainless steel belong to EET-MIC [5]. Riboflavin and FAD can accelerate electron transfer in EET-MIC. They are utilized by many microorganisms for electron transfer [36,37]. Flavins released by *Shewanella* or externally introduced can facilitate its EET because flavins function as diffusive electron shuttles [38]. Extracellular electrons from iron oxidation in Reaction (1) need to go through electron transfer consisting of the extracellular section and the intracellular section to reach the cytoplasm where they are used for the reduction reaction such as sulfate reduction in Reaction (2) or nitrate reduction [3,39]. Acceleration of either electron transfer section may result in increased overall electron transfer process [20].

Unlike iron, copper is not energetic enough as an electron donor for sulfate reduction ($E^{\circ\prime} = -217$ mV) due to the high reduction potentials of Cu^+/Cu and Cu^{2+}/Cu [40,41] in the reactions below (shown in Cu dissolution direction),

$$Cu \rightarrow Cu^+ + e^- \ (E^\circ = +520\,mV) \quad (5)$$

$$Cu \rightarrow Cu^{2+} + 2e^- \ (E^\circ = +340\,mV) \quad (6)$$

The two E° values are so high such that the very strong precipitation of Cu^+ and Cu^{2+} ions by sulfide could not shift their Nernst equations sufficiently to make Cu energetic enough for sulfate reduction. Thus, EET-MIC caused by SRB against Cu cannot happen spontaneously. However, M-MIC by HS^- can happen at neutral pH with the following reaction which has a negative Gibbs free energy change [42],

$$2Cu + HS^- + H^+ \rightarrow Cu_2S + H_{2(g)} \ (\Delta G^{\circ\prime} = -58.3\,kJ/mol) \quad (7)$$

The reaction product Cu_2S is extremely insoluble in water (pK_s 47.6 vs. 17.2 for FeS at 25°C) [43]. Its Gibbs free energy of formation ΔG_f° is −86.20 kJ/mol [42]. This very negative value contributes greatly to the negative Gibbs free energy change for Reaction (7), making this corrosion reaction thermodynamically favorable.

Because *D. vulgaris* can cause both EET-MIC of carbon steel and M-MIC of Cu, it provides an excellent model to contrast the two types of MIC mechanisms, which can help understand the two fundamental MIC mechanisms and aid in MIC forensics and mitigation strategies. Riboflavin has been used by various MIC researchers as an important probe or a tool to identify EET-MIC [33,34]. It is critically important to validate this tool by comparing its impact on EET-MIC and M-MIC.

2. Experimental

2.1. Bacterium, metals and chemicals

D. vulgaris (ATCC 7757) was cultured in modified Baar's medium (ATCC 1249 medium) [42]. The culture medium pH was adjusted to 7.0 before autoclaving. After autoclave-sterilization, the culture medium was sparged with filter-sterilized N_2 gas for 1 h to remove dissolved oxygen. Chemicals used in this study were purchased from Fisher Scientific (Pittsburgh, PA, USA) or Sigma-Aldrich (St Louis, MO, USA). X65 carbon steel (composition in [44]) and Cu (99.9 % mass purity) were cut into square coupons, each with an exposed 10 mm × 10 mm top surface. All other surfaces were protected by a Teflon paint. The top coupon surfaces were abraded to a final finish of 600-grit. They were then cleaned with pure isopropanol and dried under UV light for at least 20 min. Before inoculation, 100 mL culture medium, 20 ppm (w/w) riboflavin and 3 replicate coupons were added to each 125 mL anaerobic vial (Wheaton Industries Inc., Millville, NJ, USA) in an anaerobic chamber filled with N_2. The 1 g/L yeast extract in the culture medium is in the standard ATCC 1249 medium for optimal SRB growth. A concentrated L-cysteine stock solution was used to add 100 ppm (w/w) L-cysteine (oxygen scavenger) to the culture medium. One mL SRB seed culture was used to inoculate each vial before it was sealed with a rubber

septum and an aluminum cap. This 1 mL inoculum and 3 coupons reduced the headspace volume in each 125 mL vial from 25 mL to 23 mL. The initial planktonic cell concentration right after inoculation was about 10^5–10^6 cells/mL. All the vials were wrapped with aluminum foil to block light to protect photoactive riboflavin before they were incubated at 37 °C for 7 days.

2.2. Sessile cell counts and biofilm images

After the 7-day incubation, coupons were taken out and rinsed in a pH 7.4 phosphate buffered saline (PBS) solution 3 times. The biofilm on each coupon surface was scraped using a sterile brush into a 10 mL PBS solution and then transferred to a 50 mL conical tube and vortexed for 30 s to suspend the cells evenly in the solution. A hemocytometer was used to enumerate the sessile cell counts on the coupon surfaces of X65 carbon steel and Cu. *D. vulgaris* cells were seen as motile cells under an optical microscope at 400× magnification. The hemocytometer method requires a minimum cell count of 5×10^4 cells/mL for accuracy [18] and thus it may not be suitable for starvation or biocide kill studies. Biofilms were also examined under a scanning electron microscope (SEM) (Model JSM-6390, JEOL, Tokyo, Japan). The coupon preparation method for biofilm SEM imaging was reported before [33].

2.3. Headspace H_2 gas analysis

The H_2 concentration in the 23 mL headspace in each 125 mL anaerobic vial was measured every day during the 7-day incubation using a H_2 gas detector (Model FD-90A, Forensics Detectors, Palos Verdes Peninsula, CA, USA). Ten mL headspace gas was extracted from each 125 mL anaerobic vial using a syringe and injected into a sealed 250 mL vial filled with 1 atm air for H_2 concentration dilution. The 125 mL vial was withdrawn from incubation and the remaining replicate vials were used for headspace gas sampling for subsequent days. After dilution, 40 mL gas was withdrawn from the 250 mL dilution vial and directly injected into the H_2 detector's sampling port using a syringe without tubing. H_2S in the headspace was found not interfering with the electrochemical H_2 sensor's readings in this work.

2.4. Weight loss and pitting corrosion analyses

At least 3 coupons were used for each weight loss data point. Each coupon was weighed before and after incubation. After incubation, X65 carbon steel coupons were cleaned for 1 min using a fresh Clarke's solution to remove biofilms and corrosion products [45]. Adhering to ASTM G102 [46], a 20 % (v/v) H_2SO_4 solution was used to clean Cu coupons for 1 min. Afterwards, the X65 carbon steel and Cu coupons were rinsed with pure isopropanol and dried before weighing and corrosion pit observation under SEM. Pit depth was measured using an infinite focus microscope (IFM) profilometer (Model ALC13, Alicona Imaging GmbH, Graz, Austria). The maximum pit depths of six coupons from two replicate vials were used to provide an average maximum pit depth data point.

2.5. Electrochemical measurements

A three-electrode glass cell setup was used in this work. Each glass cell had a liquid volume of 300 mL and a headspace volume of 145 mL. A thin platinum sheet (10 mm × 10 mm × 1 mm) was used as the counter electrode, while a saturated calomel electrode (SCE) served as the reference electrode. The working electrode was either a X65 carbon steel cube or a Cu cube embedded in epoxy. Each working electrode had an exposed surface area of 1 cm^2. A VersaSTAT 3 potentiostat (Princeton Applied Research, Oak Ridge, TN, USA) was used to perform linear polarization resistance (LPR) and potentiodynamic polarization scans. The LPR's voltage range was −10 mV to 10 mV vs. the stabilized open circuit potential (OCP) at a scan rate of 0.167 mV/s. The voltage range was from −200 mV to +200 mV vs. the OCP at a scan rate of 0.167 mV/s for potentiodynamic polarization scans. For each working electrode, its potentiodynamic polarization scan was performed only once at the end of the incubation period, while LPR scans were performed once daily.

3. Results

3.1. Sessile cell counts and SEM biofilm images

Fig. 1A shows that the sessile cell counts were $(2.0 \pm 0.4) \times 10^7$ cells/cm^2 without riboflavin and $(1.9 \pm 0.6) \times 10^7$ cells/cm^2 with 20 ppm riboflavin on X65 carbon steel after the 7-day incubation. On Cu surfaces, the sessile cell counts were $(9.0 \pm 1.5) \times 10^6$ cells/cm^2 and $(6.8 \pm 2.8) \times 10^6$ cells/cm^2 without and with 20 ppm riboflavin, respectively. SEM images in Fig. 1B show that there were more sessile cells on the X65 surfaces than on the Cu surfaces. They also show that the addition of riboflavin did not visibly alter the sessile cell abundance for each metal.

3.2. H_2 concentration in headspace

Fig. 2 shows that the headspace H_2 concentrations in 125 mL anaerobic vials with and without metal coupons. It shows that in the presence of X65 carbon steel, the H_2 concentration profile during the 7-day incubation was quite close to that without coupons. On the contrary, a huge increase in H_2 concentration was observed in SRB MIC of Cu (Fig. 2). The headspace H_2 concentration with 3 Cu coupons in the broth had a peak value of 7100 ppm (v/v) vs. 1250 ppm for the coupon-free SRB broth. The headspace H_2 concentration in the abiotic control vial (with one uncoated X65 coupon in 100 mL deoxygenated culture medium at initial pH 7) in Fig. 2 exhibits a linear behavior over the 7-day incubation period. There was 1010 ppm H_2 in the 24.7 mL headspace after the 7-day incubation. The amount of H_2 was stoichiometrically equivalent to 0.054 mg Fe loss in water or proton reduction corrosion of carbon steel, amounting to 0.018 mg/cm^2 weight loss for the coupon (3 cm^2 total exposed surface) in one week, which was negligible (10^2 lower) compared with MIC weight losses.

3.3. Pit analysis and weight loss

Fig. 3(A, A′) shows that there were more and larger pits on X65 with 20 ppm riboflavin than those without. In both cases, pitting corrosion was far more severe than uniform corrosion because the parallel coupon surface polishing lines can still be seen on Fig. 3(A, A′). In comparison, the SEM images in Fig. 3(B, B′) show that the pitting corrosion severity on Cu surface did not change much by the addition of riboflavin. Furthermore, unlike in the X65 corrosion, pitting corrosion of Cu was accompanied by severe uniform corrosion that completely erased polishing lines.

The culture medium pH values after the 7-day incubation were 6.79 ± 0.05, 6.81 ± 0.07, 7.14 ± 0.01, 7.06 ± 0.03, for X65 carbon steel without and with riboflavin, Cu without and with riboflavin, respectively. These values did not deviate much from the initial pH of 7. Sulfate respiration alone does not change scalar and vectorial proton concentrations because it consumes protons released by lactate oxidation [10]. However, CO_2 from lactate oxidation can acidify the broth slightly. On the other hand, H_2S escape to the headspace increases pH [10]. The abiotic control weight losses were 0.1 mg/cm^2 and 0.3 mg/cm^2 for Cu and X65 carbon steel in the deoxygenated ATCC 1249 medium, respectively. They were much smaller than biotic weight losses in Fig. 4. Fig. 4 shows the weight losses of X65 carbon steel and Cu with and without 20 ppm riboflavin after the 7-day incubation with SRB. The biotic X65 carbon steel weight loss increased considerably from 2.5 ± 0.3 mg/cm^2 to 4.6 ± 0.1 mg/cm^2 (84 % increase) when riboflavin was added (Fig. 4A). In comparison, Fig. 4B shows that the Cu weight loss did not see a statistically significant increase with the addition of

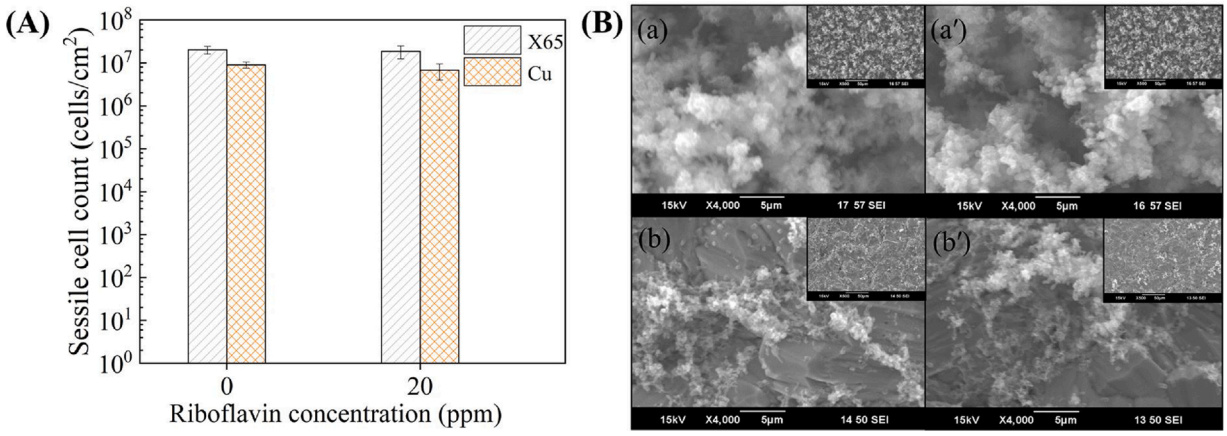

Fig. 1. (A) SRB (*D. vulgaris*) sessile cell counts of X65 carbon steel and Cu after 7-day incubation in ATCC 1249 culture medium inoculated with *D. vulgaris* with and without 20 ppm riboflavin. (Error bars stand for the standard deviations from at least three independent samples.); (B) SEM images of biofilms on X65 carbon steel and Cu surfaces after 7-day incubation with SRB: (a) X65 carbon steel without riboflavin, (a′) X65 carbon steel with 20 ppm riboflavin, (b) Cu without riboflavin, (b′) Cu with 20 ppm riboflavin.

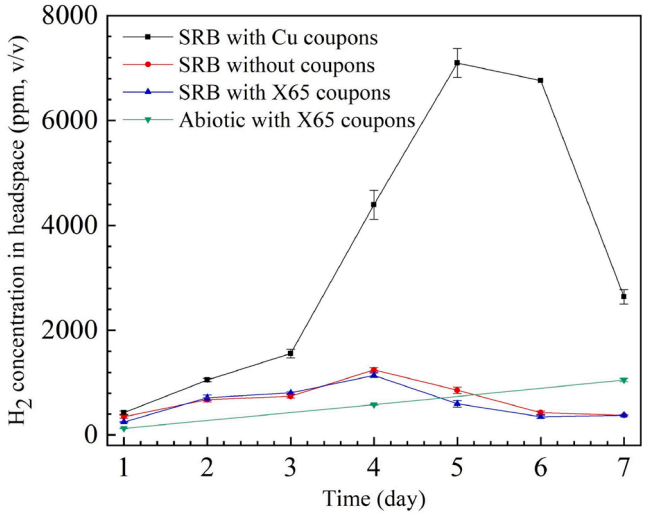

Fig. 2. H_2 concentration in the headspace of each 125 mL anaerobic vial with and without 3 metal coupons during the 7-day incubation with SRB.

riboflavin (28.7 ± 3.8 mg/cm^2 vs. 32.5 ± 7.2 mg/cm^2, p-value = 0.50).

The average maximum pit depths of X65 carbon steel and Cu with and without 20 ppm riboflavin after the 7-day incubation are shown in Fig. 5. For X65 carbon steel, it increased considerably from 6.6 ± 0.4 μm to 18.8 ± 0.7 μm with the addition of riboflavin. In comparison, for Cu, it did not increase statistically (22.7 ± 4.5 μm vs. 24.3 ± 4.6 μm, p-value = 0.70).

3.4. Electrochemical measurements

Weight loss and pit depth data reflect cumulative effects because they take a significant lead time to be measurable. Electrochemical measurements can provide useful transient data start from the beginning of incubation. Fig. 6 shows the daily OCP data for X65 carbon steel and Cu MIC by *D. vulgaris* with and without 20 ppm riboflavin in the culture medium. The OCP values for X65 carbon steel was largely unaffected by the addition of 20 ppm riboflavin. They had a slight increase during the 7-day incubation period. The OCP values for Cu with and without 20 ppm riboflavin were similar and they stayed near −0.8 V (vs. SCE) between days 2 and 7 after a drop of around 0.12 V in the first day.

Polarization resistances (R_p) were recorded for both X65 carbon steel and Cu with and without 20 ppm riboflavin during the 7-day incubation (Fig. 7). R_p of X65 carbon steel peaked on days 4 and 5 with and without 20 ppm riboflavin, respectively. The R_p curve without riboflavin was much higher than that with 20 ppm riboflavin. In comparison, for Cu MIC, the curves with and without riboflavin were close to each other.

Potentiodynamic polarization was performed at the end of incubation to obtain corrosion current density (i_{corr}) data, which can be used to calculate corrosion rates directly to support weigh loss data trend. Fig. 8 shows the potentiodynamic polarization curves of X65 carbon steel and Cu with and without 20 ppm riboflavin. Table 1 lists the electrochemical parameters derived from the Tafel analysis of the curves in Fig. 8. It shows that i_{corr} of X65 carbon steel increased from 12 μA/cm^2 to 23 μA/cm^2 (92 % increase) with the addition of 20 ppm riboflavin. In comparison, i_{corr} of Cu had only a slight increase from 27 μA/cm^2 to 31 μA/cm^2.

4. Discussion

Fig. 1A indicates that 20 ppm riboflavin did not lead to statistically significant increase of the sessile cell counts on X65 carbon steel (p-value = 0.78) and Cu (p-value = 0.58). The addition of 20 ppm riboflavin increased the energy harvest rate from elemental iron via EET [3]. This led to more severe corrosion of X65 carbon steel. However, Cu MIC by *D. vulgaris* did not benefit from 20 ppm riboflavin because its mechanism belongs to M-MIC. The yeast extract in the ATCC 1249 medium contains less than 0.1 ppm riboflavin, a negligible amount compared to the 20 ppm added in this work. It is beneficial to grow a pure-strain SRB in a standard medium to study SRB MIC mechanisms for better comparison and less complication.

Because H_2 is a low molecular weight gas with a negligible solubility, H_2 evolution is very sensitive in corrosion processes that produce H_2. The negligible 7-day carbon steel corrosion of 0.018 mg/cm^2 weight loss in the abiotic culture medium (initial pH 7) generated 1010 ppm H_2 in the headspace, which is much higher than the H_2 sensor's detection limit of 1 ppm. This means that H_2 concentrations corresponding to microgram weight losses can be measured. This is 10^2-10^3 more sensitive than weighing coupons. Thus, H_2 detection in a sealed system is a powerful tool in detecting corrosion that generates H_2, including corrosion by CO_2, H_2S, and organic acids.

In the following reaction of H_2S corrosion of carbon steel, 1 mg Fe weight loss generates 0.018 mmol of H_2 stoichiometrically. This small 1 mg weight loss would increase the H_2 concentration by 1.9×10^4 ppm in the 23 mL headspace at 37 °C and 1 atm.

$$Fe + HS^- + H^+ \rightarrow FeS + H_{2(g)} \quad (8)$$

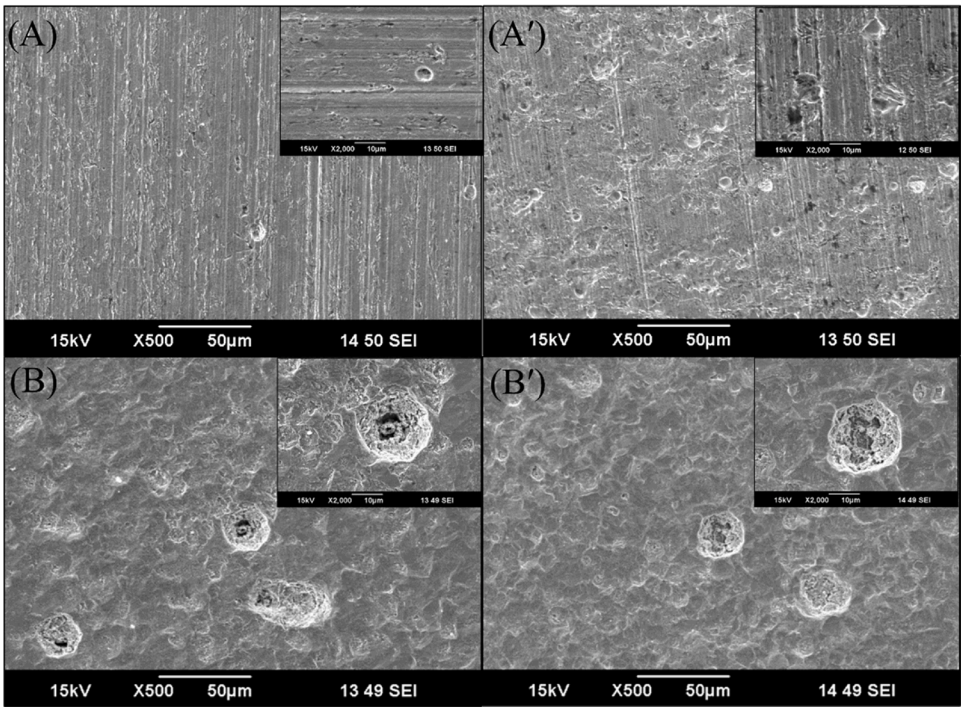

Fig. 3. Pit morphology on X65 carbon steel and Cu surfaces after 7-day incubation with SRB: (A) X65 carbon steel without riboflavin, (A′) X65 carbon steel with 20 ppm riboflavin, (B) Cu without riboflavin, (B′) Cu with 20 ppm riboflavin.

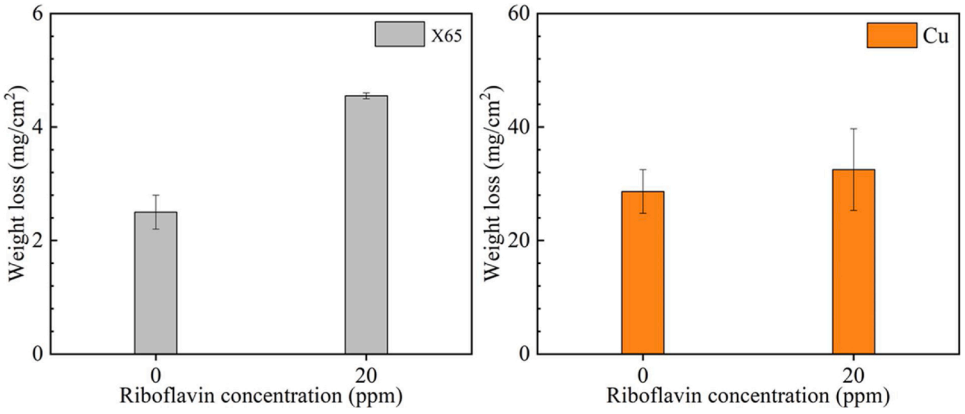

Fig. 4. Weight losses of X65 carbon steel and Cu coupons after the 7-day incubation with SRB. (Error bars stand for the standard deviations from at least three independent samples.).

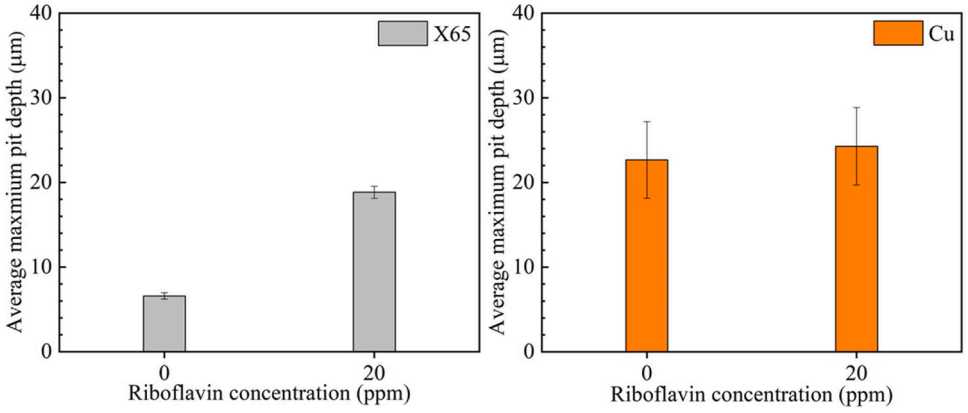

Fig. 5. Pit depth of X65 carbon steel and Cu coupons after the 7-day incubation with SRB. (Error bars stand for the standard deviations from at least three coupons.).

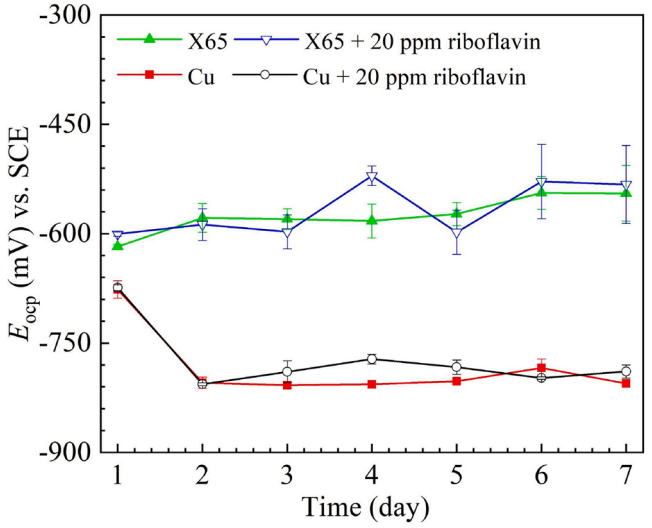

Fig. 6. OCP vs. time during the 7-day incubation with and without 20 ppm riboflavin in the SRB broths. (Error bars stand for the standard deviations from three independent samples.).

Fig. 2 indicates that the headspace H_2 concentration profiles with X65 carbon steel coupons and without any coupons were practically the same. This effectively rules out biogenic H_2S corrosion of carbon steel as a significant mechanism for the SRB MIC of carbon steel in this work. This observation lends a direct and strong support to the conclusion by Jia et al. [18,10] that H_2S was not a significant contributor to SRB MIC of carbon steel at near neutral pH, because the corrosion mechanism is EET-MIC, rather than M-MIC by H_2S.

In comparison, the huge increase (up to 5.7-fold at peak values) in the headspace H_2 concentration in the presence of Cu coupons in Fig. 2 supported the M-MIC mechanism of Cu in Reaction (7), which indicates that 1 mg of Cu weight loss corresponds to 0.0079 mmol of H_2 generation stoichiometrically. It would be ideal if H_2 evolution can be used to calculate Cu weight loss quantitatively using this stoichiometry. However, *D. vulgaris* is known to produce H_2 from lactate oxidation as shown in the following reaction [47],

$$CH_3CHOHCOO\ (\text{Lactate}) + 2H_2O \rightarrow CH_3COO\ (\text{Acetate}) + 2.5H_2 + HCO_3 \quad (9)$$

This is confirmed by the bell-shaped H_2 evolution profile for the SRB broth without coupons in Fig. 2. *D. vulgaris* consumes H_2 as an energy source when lactate is in short supply [47]

$$SO_4^{2-}\ (\text{Sulfate}) + 5H_2 \rightarrow H_2S + 4H_2O \quad (10)$$

All the three biotic H_2 profiles in Fig. 2 exhibit a bell-shape, suggesting initial generation and later consumption of H_2 by *D. vulgaris*.

Fig. 5 shows that the average maximum pit depth with 20 ppm riboflavin was 2.8 times of that without riboflavin for X65 carbon steel, indicating that the electron mediator made the pitting corrosion far more severe. In comparison, there was no statistically significant increase in pitting corrosion severity for Cu. The pit images in Fig. 3 corroborate the pit depth data trends.

The abiotic control weight losses for Cu and X65 (0.1 mg/cm^2 and 0.3 mg/cm^2, respectively) were practically negligible compared to the much larger biotic weight losses (Fig. 4). This was because without SRB biocatalysis, the deoxygenated abiotic culture medium did not have a utilizable electron acceptor to cause corrosion. The abiotic weight losses were found practically unaffected by the addition of 20 ppm riboflavin

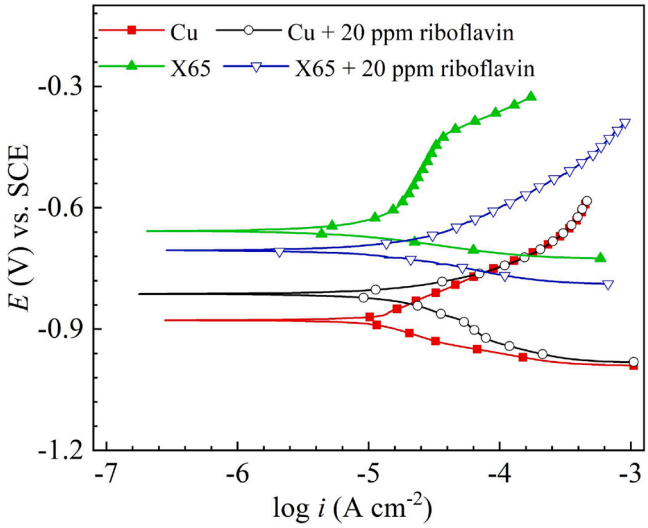

Fig. 8. Potentiodynamic polarization curves of X65 carbon steel and Cu in SRB broths after the 7-day incubation with and without 20 ppm riboflavin.

Table 1
The fitted polarization parameters of X65 steel and Cu in *D. vulgaris* with 0 ppm and 20 ppm riboflavin after 7-day incubation.

	i_{corr} (μA/cm^2)	E_{corr} vs. SCE (V)	β_a (V/dec)	β_c (V/dec)
X65 + 0 ppm riboflavin	12	−0.66	0.34	0.06
X65 + 20 ppm riboflavin	23	−0.71	0.16	0.10
Cu + 0 ppm riboflavin	27	−0.88	0.27	0.16
Cu + 20 ppm riboflavin	31	−0.81	0.10	0.26

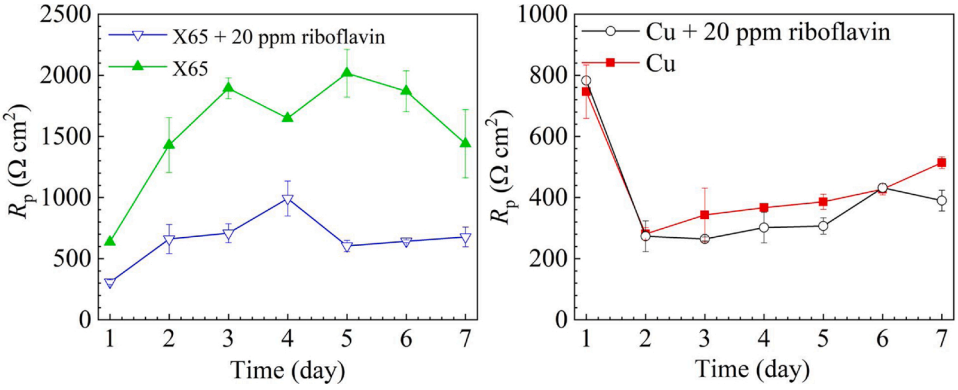

Fig. 7. Variations of R_p vs. time of (A) X65 carbon steel, (B) Cu during the 7-day incubation with and without 20 ppm riboflavin in SRB broths. (Error bars represent standard deviations from three independent runs.).

for Cu (0.1 mg/cm^2 vs. 0.1 mg/cm^2 after addition) and X65 carbon steel (0.3 mg/cm^2 vs. 0.2 mg/cm^2 after addition). In the presence of SRB, the addition of riboflavin caused an 84 % weight loss increase for X65 carbon steel corrosion after the 7-day incubation (Fig. 4), suggesting that riboflavin accelerated electron transfer, which is rate limiting in EET-MIC by *D. vulgaris* against X65 carbon steel [3]. In comparison, for Cu MIC by *D. vulgaris*, the weight loss increase was statistically insignificant (p-value 0.49). This means 20 ppm riboflavin did not enhance Cu MIC by *D. vulgaris*, which confirms that Cu MIC by SRB is not EET-MIC.

It is important to note that the Cu weight loss was an order of magnitude larger than that of X65 carbon steel (Fig. 4). For X65 carbon steel, parallel polishing lines are still visible after incubation in Fig. 3(A, A′). In comparison, the polishing lines are completely absent for Cu after the 7-day incubation in Fig. 3(B, 4B′), suggesting that a surface layer was completely removed by corrosion.

In EET-MIC, sessile cells utilize electrons from extracellular iron oxidation via EET for sulfate reduction, which produces energy. EET-MIC is limited to the energy need for the sessile cells to survive. Planktonic cells do not get the energy. Thus, the extent of MIC is rather limited. However, this is not true for M-MIC. Both sessile and planktonic SRB cells produce H_2S. Therefore, Cu weight loss due to H_2S corrosion can be much larger than carbon steel weight loss for SRB corrosion as evidenced by the 10^1 higher weight loss for Cu than that for X65 carbon steel in Fig. 4. Fig. 9 is a schematic comparison of EET-MIC of Fe and M-MIC of Cu by a *D. vulgaris* biofilm. The exact mechanisms of how riboflavin shuttles extracellular, and perhaps also intracellular electrons, remain to be elucidated by bio-scientists.

A more negative OCP indicates a higher thermodynamic tendency for the working electrode to lose electrons in the open circuit condition. During the 7-day incubation, the OCP curves for Cu were much lower than those of X65 carbon steel (Fig. 6). The OCP values for Cu in the SRB broth here were consistent with the observation by Chen et al., who found that Cu's OCP was −925 mV (vs. SCE) in 0.1 M NaCl + 5×10^{-4} M Na_2S solution [48], reflecting a 700 mV drop from Cu's OCP of −225 mV (vs. SCE) in 0.1 M NaCl [49]. They attributed this large decrease of OCP to the extremely low solubility of Cu_2S, which lowered the dissolved Cu ion concentration. For X65, with and without riboflavin addition, the OCP curves are quite close in Fig. 6, suggesting that riboflavin did not change the thermodynamic driving force in X65 MIC. This was consistent with the kinetic role of riboflavin as an electron mediator that accelerated X65 MIC by enhancing EET.

For Cu MIC, the two R_p curves in Fig. 7B had a large decrease from day 1 to day 2, indicating a large increase in corrosion rate. This interesting phenomenon can be explained by the fact that as incubation time increased more H_2S (corrosive metabolite) was secreted by the *D. vulgaris* cells. However, during the same time period, an increase is seen for the two R_p curves for X65 MIC in Fig. 7A. This can be explained by the build-up of an iron sulfide film on X65 that offered partial passivation. Fig. 7A shows that 20 ppm riboflavin caused the R_p curves of X65 carbon steel to shift much lower during the entire 7-day incubation period, which means corrosion resistance was much reduced. In comparison, 20 ppm riboflavin did not reduce the Cu corrosion resistance (Fig. 7B). The impact of riboflavin on corrosion rate reflected by the LPR data here is clearly consistent with the weight loss data above.

The i_{corr} data in Table 1 from the Tafel analysis of the potentiodynamic polarization curves (Fig. 8) at the end of the 7-day incubation show a 97 % increase for X65 carbon steel when riboflavin was added. In comparison, the increase of i_{corr} for Cu was only 15 %. The corrosion trends based on i_{corr} corroborated the corrosion trends in weight loss data for both X65 carbon steel and Cu. Note that i_{corr} only reflected the corrosion rate at the end of the incubation period, rather than the entire 7-day incubation period. Unlike LPR, the voltage range in potentiodynamic polarization is typically much larger, which can alter the working electrode's surface properties. Thus, potentiodynamic polarization is usually scanned once at the end of an experiment [50].

In this work, Cu corrosion was rather severe with surface thickness loss due to uniform corrosion (also known as general corrosion) as shown in SEM images (Fig. 3). In such an MIC case, pitting corrosion characterization alone grossly underestimates corrosion severity. This is because pit depth starting from the corroded surface rather than from the uncorroded surface does not account for the fact that corrosion removes a substantial layer from a coupon surface. Thus, both pit depth and weight loss must be used to describe corrosion severity. A uniform corrosion rate can be calculated based on the weight loss using a simple mass balance. However, this corrosion rate does not reflect pitting damages. Recently, Dou et al. used relative pitting severity (*RPS*) to reflect the relative importance of pitting corrosion to uniform corrosion [42]. *RPS* is the ratio of pit growth rate to (uniform) corrosion rate based on specific weight loss, which can be calculated from the following equation,

$$RPS = \frac{\text{(average) maximum pit depth} \times \text{metal density}}{\text{average specific weight loss}} \tag{11}$$

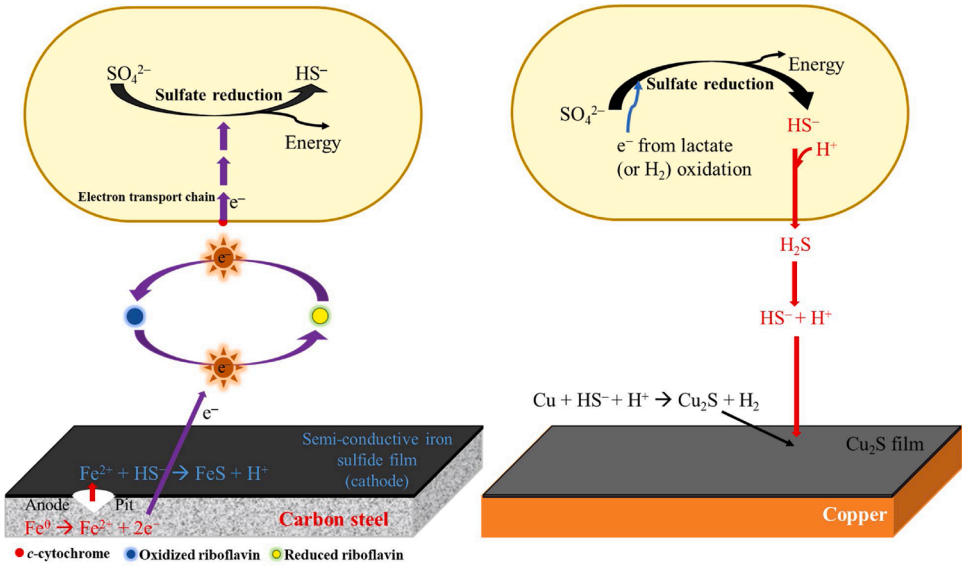

Fig. 9. Schematic of a comparison of EET-MIC of Fe with riboflavin as an electron mediator and M-MIC of Cu by *D. vulgaris* biofilm.

$$\{ \text{RPS} \gg 1, \quad \text{pitting corrosion is much more severe than uniform corrosion} \tag{12a}$$

$$\{ \text{RPS} \approx 1, \quad \text{pitting corrosion and uniform corrosion are equally important} \tag{12b}$$

$$\{ \text{RPS} \ll 1, \quad \text{uniform corrosion is much more severe than pitting corrosion} \tag{12c}$$

RPS can be used together with either pit depth data or weight loss data to describe corrosion severity adequately. The maximum pit growth rate was calculated using the average of several deepest pits in this work. For the criteria in Eq. (12), pit depth is measured from the corroded surface, rather than the uncorroded surface used in pitting factor, which is not convenient to measure in short-term lab tests.

RPS can provide an insight into the rather striking behavioral differences between the two MIC cases in this work. For X65 carbon steel MIC by *D. vulgaris*, the average maximum pit depth (Fig. 5) and weight loss (Fig. 4) without 20 ppm riboflavin were 6.6 μm and 2.5 mg/cm^2, respectively after the 7-day incubation. Thus, the *RPS* value was 2.1 according to Eq. (11) by using X65 carbon steel density of 7.87 g/cm^3. With the addition of 20 ppm riboflavin, the *RPS* increased to 3.2. Both *RPS* values are considerably larger than unity, which means pitting corrosion was more severe than uniform corrosion. An oilfield biofilm consortium grown in enriched artificial seawater with FeS precipitation corroded carbon steel with a narrow *RPS* value range of 3.5–3.7 in enriched artificial seawater after 60 days of incubation with and without biocide treatment [51].

Cu MIC in this work, *RPS* values were 0.67 and 0.71 with and without 20 ppm riboflavin, respectively. They considerably smaller than unity, suggesting that uniform corrosion was more severe in Cu MIC by *D. vulgaris*. The two small *RPS* values indicate that the losses of Cu coupon surface thicknesses were significantly larger than their corresponding average maximum pit depths according to Eq. (12a). The very different *RPS* values between the X65 carbon steel and Cu systems are another clear indication that their *D. vulgaris* corrosion mechanisms are fundamentally different.

Cu ions, even at very low concentrations, are cytotoxic to microorganisms [52]. Cu has been used as an alloying element to produce Cu-bearing stainless steels that release Cu ions upon corrosion by microbes. The released Cu ions have been shown to prevent further MIC by *P. aeruginosa* [53]. However, *D. vulgaris* sessile cells formed robust biofilms on Cu in this work as shown in Fig. 1. This means *D. vulgaris* overcame the inhibition by copper, because *D. vulgaris* produced sulfides that precipitated microbiocidal Cu^+ to form extremely insoluble Cu_2S [54].

5. Conclusion

The experimental results in this work revealed that 20 ppm riboflavin accelerated X65 carbon steel MIC by *D. vulgaris* considerably, but it did not enhance Cu MIC by the same SRB, thus validating the electron mediator as a tool to distinguish EET-MIC from M-MIC. Cu MIC had much lower *RPS* values than X65 carbon steel MIC, suggesting that their corresponding MIC mechanisms are fundamentally different. This MIC science study confirmed that electron transfer is rate limiting in X65 carbon steel MIC by *D. vulgaris*, but it is not the case for Cu MIC by *D. vulgaris* because the former belongs to EET-MIC, while the latter is M-MIC. This specially designed "one microbe two metals" work presented an interesting case in which even with the same microbe in the same culture medium, two very different MIC mechanisms occurred for two different metals with very different corrosion characteristics. This work also demonstrated that headspace H_2 monitoring is a powerful tool that can help confirm corrosion reactions with H_2 evolution, which is common in M-MIC.

CRediT authorship contribution statement

Di Wang: Investigation, Writing - original draft, Methodology. **Jialin Liu:** Investigation, Writing - original draft, Methodology. **Ru Jia:** Methodology, Resources. **Wenwen Dou:** Methodology, Resources. **Sith Kumseranee:** Project administration, Funding acquisition. **Suchada Punpruk:** Project administration, Funding acquisition. **Xiaogang Li:** Project administration, Funding acquisition. **Tingyue Gu:** Conceptualization, Methodology, Writing - review & editing, Supervision, Funding acquisition.

Declaration of Competing Interest

The authors declare that they have no known competing financial interests or personal relationships that could have appeared to influence the work reported in this paper.

Acknowledgements

We thank NACE International (Houston, TX) for the permission to use a small part of Corrosion/2018 conference Paper No. 10586 in this journal paper. This work was supported by PTT Exploration and Production, Thailand and Chinese Society for Corrosion and Protection. WD thanks the China Scholarship Council for financial support for studying in USA.

References

[1] K.M. Al-Nabulsi, F.M. Al-Abbas, T.Y. Rizk, A.E.M. Salameh, Microbiologically assisted stress corrosion cracking in the presence of nitrate reducing bacteria, Eng. Fail. Anal. 58 (2015) 165–172.
[2] B.J. Little, D.J. Blackwood, J. Hinks, F.M. Lauro, E. Marsili, A. Okamoto, S.A. Rice, S.A. Wade, H.-C. Flemming, Microbially influenced corrosion—Any progress? Corros. Sci. 170 (2020), 108641. In Press.
[3] T. Gu, R. Jia, T. Unsal, D. Xu, Toward a better understanding of microbiologically influenced corrosion caused by sulfate reducing bacteria, J. Mater. Sci. Technol. 35 (2019) 631–636.
[4] M.K. Schütz, M.L. Schlegel, M. Libert, O. Bildstein, Impact of iron-reducing bacteria on the corrosion rate of carbon steel under simulated geological disposal conditions, Environ. Sci. Technol. 49 (2015) 7483–7490.
[5] Y. Li, D. Xu, C. Chen, X. Li, R. Jia, D. Zhang, W. Sand, F. Wang, T. Gu, Anaerobic microbiologically influenced corrosion mechanisms interpreted using bioenergetics and bioelectrochemistry: a review, J. Mater. Sci. Technol. 34 (2018) 1713–1718.
[6] R. Jia, D. Yang, D. Xu, T. Gu, Carbon steel biocorrosion at 80 °C by a thermophilic sulfate reducing archaeon biofilm provides evidence for its utilization of elemental iron as electron donor through extracellular electron transfer, Corros. Sci. 145 (2018) 47–54.
[7] R. Jia, D. Yang, J. Xu, D. Xu, T. Gu, Microbiologically influenced corrosion of C1018 carbon steel by nitrate reducing *Pseudomonas aeruginosa* biofilm under organic carbon starvation, Corros. Sci. 127 (2017) 1–9.
[8] G. Reguera, K.D. McCarthy, T. Mehta, J.S. Nicoll, M.T. Tuominen, D.R. Lovley, Extracellular electron transfer via microbial nanowires, Nature. 435 (2005) 1098–1101.
[9] E. Marsili, D.B. Baron, I.D. Shikhare, D. Coursolle, J.A. Gralnick, D.R. Bond, Shewanella secretes flavins that mediate extracellular electron transfer, Proc. Natl. Acad. Sci. 105 (2008) 3968–3973.
[10] R. Jia, J.L. Tan, P. Jin, D.J. Blackwood, D. Xu, T. Gu, Effects of biogenic H_2S on the microbiologically influenced corrosion of C1018 carbon steel by sulfate reducing *Desulfovibrio vulgaris* biofilm, Corros. Sci. 130 (2018) 1–11.
[11] W. Dou, J. Liu, W. Cai, D. Wang, R. Jia, S. Chen, T. Gu, Electrochemical investigation of increased carbon steel corrosion via extracellular electron transfer by a sulfate reducing bacterium under carbon source starvation, Corros. Sci. 150 (2019) 258–267.
[12] D. Xu, Y. Li, F. Song, T. Gu, Laboratory investigation of microbiologically influenced corrosion of C1018 carbon steel by nitrate reducing bacterium *Bacillus licheniformis*, Corros. Sci. 77 (2013) 385–390.
[13] J. Philips, N.V. den Driessche, K.D. Paepe, A. Prévoteau, J.A. Gralnick, J.B. A. Arends, K. Rabaey, A novel *Shewanella* isolate enhances corrosion by using metallic iron as the electron donor with fumarate as the electron acceptor, Appl. Environ. Microbiol. 84 (2018).
[14] D. Xu, T. Gu, Carbon source starvation triggered more aggressive corrosion against carbon steel by the *Desulfovibrio vulgaris* biofilm, Int. Biodeterior. Biodegrad. 91 (2014) 74–81.
[15] P. Zhang, D. Xu, Y. Li, K. Yang, T. Gu, Electron mediators accelerate the microbiologically influenced corrosion of 304 stainless steel by the *Desulfovibrio vulgaris* biofilm, Bioelectrochemistry. 101 (2015) 14–21.

[16] R.K. Thauer, E. Stackebrandt, W.A. Hamilton, Energy metabolism and phylogenetic diversity of sulphate-reducing bacteria, in: L.L. Barton, W.A. Hamilton (Eds.), Sulphate-Reducing Bacteria: Environmental and Engineered Systems, Cambridge University Press, Cambridge, UK, 2007, pp. 1–37.
[17] P. Elliott, S. Ragusa, D. Catcheside, Growth of sulfate-reducing bacteria under acidic conditions in an upflow anaerobic bioreactor as a treatment system for acid mine drainage, Water Res. 32 (1998) 3724–3730.
[18] R. Jia, D. Wang, P. Jin, T. Unsal, D. Yang, J. Yang, D. Xu, T. Gu, Effects of ferrous ion concentration on microbiologically influenced corrosion of carbon steel by sulfate reducing bacterium *Desulfovibrio vulgaris*, Corros. Sci. 153 (2019) 127–137.
[19] S. Kato, Microbial extracellular electron transfer and its relevance to iron corrosion, Microb. Biotechnol. 9 (2016) 141–148.
[20] C.I. Torres, A.K. Marcus, H.-S. Lee, P. Parameswaran, R. Krajmalnik-Brown, B. E. Rittmann, A kinetic perspective on extracellular electron transfer by anode-respiring bacteria, FEMS Microbiol. Rev. 34 (2010) 3–17.
[21] F. Aulenta, A. Catervi, M. Majone, S. Panero, P. Reale, S. Rossetti, Electron transfer from a solid-state electrode assisted by methyl viologen sustains efficient microbial reductive dechlorination of TCE, Environ. Sci. Technol. 41 (2007) 2554–2559.
[22] K.M. Usher, A.H. Kaksonen, I. Cole, D. Marney, Critical review: microbially influenced corrosion of buried carbon steel pipes, Int. Biodeterior. Biodegrad. 93 (2014) 84–106.
[23] X. Deng, N. Dohmae, K.H. Nealson, K. Hashimoto, A. Okamoto, Multi-heme cytochromes provide a pathway for survival in energy-limited environments, Sci. Adv. 4 (2018) eaao5682.
[24] Y. Tokunou, K. Hashimoto, A. Okamoto, Acceleration of extracellular electron transfer by alternative redox-active molecules to riboflavin for outer-membrane cytochrome *c* of *Shewanella oneidensis* MR-1, J. Phys. Chem. C. 120 (2016) 16168–16173.
[25] X. Deng, N. Dohmae, A.H. Kaksonen, A. Okamoto, Biogenic iron sulfide nanoparticles to enable extracellular electron uptake in sulfate-reducing bacteria, Angew. Chem. Int. Ed. 59 (2020) 5995–5999.
[26] D.R. Noguera, G.A. Brusseau, B.E. Rittmann, D.A. Stahl, A unified model describing the role of hydrogen in the growth of *Desulfovibrio vulgaris* under different environmental conditions, Biotechnol. Bioeng. 59 (1998) 732–746.
[27] G. Voordouw, Molecular biology of the sulfate-reducing bacteria. Sulfate-Reducing Bact. Contemp. Perspect, Springer, 1993, pp. 88–130.
[28] W. Lubitz, H. Ogata, O. Rüdiger, E. Reijerse, Hydrogenases, Chem. Rev. 114 (2014) 4081–4148.
[29] Y. Feng, R.P. Swenson, Evaluation of the role of specific acidic amino acid residues in electron transfer between the flavodoxin and cytochrome c_3 from *Desulfovibrio vulgaris* [Hildenborough], Biochemistry. 36 (1997) 13617–13628.
[30] S.-H. Jung, Y.-H. Ahn, S.-E. Oh, J.-H. Lee, K.-T. Cho, Y.-J. Kim, M.-W. Kim, J.-M. Shim, M.-S. Kang, Impedance and thermodynamic analysis of bioanode, abiotic anode, and riboflavin-amended anode in microbial fuel cells, Bull. Korean Chem. Soc. 33 (2012) 3349–3354.
[31] H.D. Peck, Bioenergetic strategies of the sulfate-reducing bacteria, in: J.M. Odom, R. Singleton (Eds.), Sulfate-Reducing Bact. Contemp. Perspect., Springer New York, New York, NY, 1993, pp. 41–76.
[32] L. Huang, J. Tang, M. Chen, X. Liu, S. Zhou, Two modes of riboflavin-mediated extracellular electron transfer in *Geobacter uraniireducens*, Front. Microbiol. 9 (2018).
[33] R. Jia, D. Yang, D. Xu, T. Gu, Electron transfer mediators accelerated the microbiologically influence corrosion against carbon steel by nitrate reducing *Pseudomonas aeruginosa* biofilm, Bioelectrochemistry. 118 (2017) 38–46.
[34] H. Li, D. Xu, Y. Li, H. Feng, Z. Liu, X. Li, T. Gu, K. Yang, Extracellular electron transfer is a bottleneck in the microbiologically influenced corrosion of C1018 carbon steel by the biofilm of sulfate-reducing bacterium *Desulfovibrio vulgaris*, PLoS One 10 (2015) 1–12.
[35] Y. Huang, E. Zhou, C. Jiang, R. Jia, S. Liu, D. Xu, T. Gu, F. Wang, Endogenous phenazine-1-carboxamide encoding gene PhzH regulated the extracellular electron transfer in biocorrosion of stainless steel by marine *Pseudomonas aeruginosa*, Electrochem. Commun. 94 (2018) 9–13.
[36] C.A. Abbas, A.A. Sibirny, Genetic control of biosynthesis and transport of riboflavin and flavin nucleotides and construction of robust biotechnological producers, Microbiol. Mol. Biol. Rev. 75 (2011) 321–360.
[37] A. Bacher, S. Eberhardt, M. Fischer, K. Kis, G. Richter, Biosynthesis of vitamin B2 (riboflavin), Annu. Rev. Nutr. 20 (2000) 153–167.
[38] L. Shi, H. Dong, G. Reguera, H. Beyenal, A. Lu, J. Liu, H.-Q. Yu, J.K. Fredrickson, Extracellular electron transfer mechanisms between microorganisms and minerals, Nat. Rev. Microbiol. 14 (2016) 651.
[39] C. Zhao, J. Wu, Y. Ding, V.B. Wang, Y. Zhang, S. Kjelleberg, J.S.C. Loo, B. Cao, Q. Zhang, Hybrid conducting biofilm with built-in bacteria for high-performance microbial fuel cells, ChemElectroChem. 2 (2015) 654–658.
[40] J. Tomasi, B. Mennucci, R. Cammi, Quantum mechanical continuum solvation models, Chem. Rev. 105 (2005) 2999–3094.
[41] W. Fu, Y. Li, D. Xu, T. Gu, Comparing two different types of anaerobic copper biocorrosion by sulfate- and nitrate-reducing bacteria, Mater. Perform. 53 (2014) 66–70.
[42] W. Dou, R. Jia, P. Jin, J. Liu, S. Chen, T. Gu, Investigation of the mechanism and characteristics of copper corrosion by sulfate reducing bacteria, Corros. Sci. 144 (2018) 237–248.
[43] J.F. Blais, Z. Djedidi, CheikhR. Ben, R.D. Tyagi, G. Mercier, Metals precipitation from effluents: review, Pract. Period. Hazard. Toxic Radioact. Waste Manag. 12 (2008) 135–149.
[44] J. Liu, W. Dou, R. Jia, S. Kumseranee, S. Punpruk, T. Gu, *Desulfovibrio vulgaris* corroded X65 carbon steel and copper with two different types of MIC mechanisms, *Desulfovibrio vulgaris* corroded X65 carbon steel and copper with two different types of MIC mechanisms. Corrosion/2018 Paper No. 10586, NACE International, Phoenix, AZ, USA, 2018.
[45] ASTM G1-03, Standard Practice for Preparing, Cleaning and Evaluating Corrosion Test Specimens, 2003.
[46] ASTM G102-89, Calculation of Corrosion Rates and Related Information From Electrochemical Measurements, 2004.
[47] N.W. Smith, P.R. Shorten, E. Altermann, N.C. Roy, W.C. McNabb, A mathematical model for the hydrogenotrophic metabolism of sulphate-reducing bacteria, Front. Microbiol. 10 (2019).
[48] J. Chen, Z. Qin, D.W. Shoesmith, Kinetics of corrosion film growth on copper in neutral chloride solutions containing small concentrations of sulfide, J. Electrochem. Soc. 157 (2010) C338–C345.
[49] S. Zor, Sulfathiazole as potential corrosion inhibitor for copper in 0.1 M NaCl, Prot. Met. Phys. Chem. Surf. 50 (2014) 530–537.
[50] R.A. Buchanan, E.E. Stansbury, Electrochemical corrosion, in: M. Kutz (Ed.), Handbook of Environmental Degradation of Materials, William Andrew Publishing, Oxford, 2005, pp. 81–103.
[51] D. Wang, M. Ramadan, S. Kumseranee, S. Punpruk, T. Gu, Mitigating microbiologically influenced corrosion of an oilfield biofilm consortium on carbon steel in enriched hydrotest fluid using 2,2-dibromo-3-nitrilopropionamide (DBNPA) enhanced by a 14-mer peptide, J. Mater. Sci. Technol. 57 (2020) 146–152.
[52] S. Mathews, M. Hans, F. Mücklich, M. Solioz, Contact killing of bacteria on copper is suppressed if bacterial-metal contact is prevented and is induced on iron by copper ions, Appl. Environ. Microbiol. 79 (2013) 2605–2611.
[53] D. Xu, E. Zhou, Y. Zhao, H. Li, Z. Liu, D. Zhang, C. Yang, H. Lin, X. Li, K. Yang, Enhanced resistance of 2205 Cu-bearing duplex stainless steel towards microbiologically influenced corrosion by marine aerobic *Pseudomonas aeruginosa* biofilms, J. Mater. Sci. Technol. 34 (2018) 1325–1336.
[54] D. Shea, G.R. Helz, The solubility of copper in sulfidic waters: sulfide and polysulfide complexes in equilibrium with covellite, Geochim. Cosmochim. Acta 52 (1988) 1815–1825.